CHARGED VETO SIMULATIONS

M. Blecher, Virginia Tech, January, 2001

A geant simulation of a charged veto system has been carried out. The geometry includes the vacuum tank, up and down stream eye shaped beam pipes, and surrounding side, top/bottom, upstream, and gap vetos. The figures for all of these were shown during the last December, 2000 collaboration meeting. They are available at our web site under, New GEANT schematics "M. Blecher figures." What I have added in the way of additional charged particle vetos inside the vacuum tank are two layers of 1 mm thick scintillators which line the inside of the vacuum tank. Those lining the middle cylinder are numbered 1 and 2, those lining the downstream (upstream) hemispheres are numbered 3 and 4, (5 and 6). The lower number of the pair is the outer scintillator.

The simulation begins by transporting $10^6$ $K_L$ from the production target at $z = -12$ m to some point inside the vacuum tank with the proper life time distribution. The mean momentum was $P_K = 0.750$ GeV with $\sigma = 0.200$ GeV. In figure 1, The xy spot size at the decay point is shown in the top left scatterplot, the z position relative to the vacuum tank center is shown in the top right histogram, the $K_L$ momentum and its time-of-flight to the decay point are shown in the bottom left and right histograms.

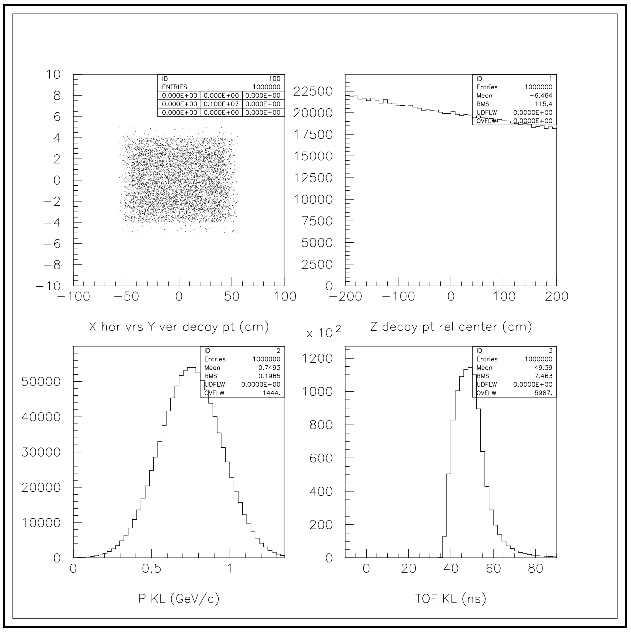


FIG. 1. Specification of $K_L$ position and kinematics at decay point.

The outer scatterplot entries are due to the bin sizes.

At this point the decay $K_L \to \pi^- e^+ \nu \gamma$ is forced to occur. The decay particles are numbered, for future reference, as follows: $\pi = 1$, $e = 2$, $\nu = 3$, and $\gamma = 4$. The CM kinematics were generated by GENBOD and weighted by the matrix element using the function WL3G obtained from D. Jaffe through A. Konaka. It should be noted that this function is not completely correct since it sometimes spits out a negative weight. The CM kinetic energies are shown in figure 2. There are more than $10^6$ entries as sometimes the event is rejected because the chosen random number is greater than the weight, while the event is entered into the histogram with the weight before the rejection test. Thus these distributions are correct and use all the statistics. Note the weighting function rejects events with $\mathrm{KE}_\gamma < 30$ MeV and $\cos\theta_{e\gamma} < 20°$.

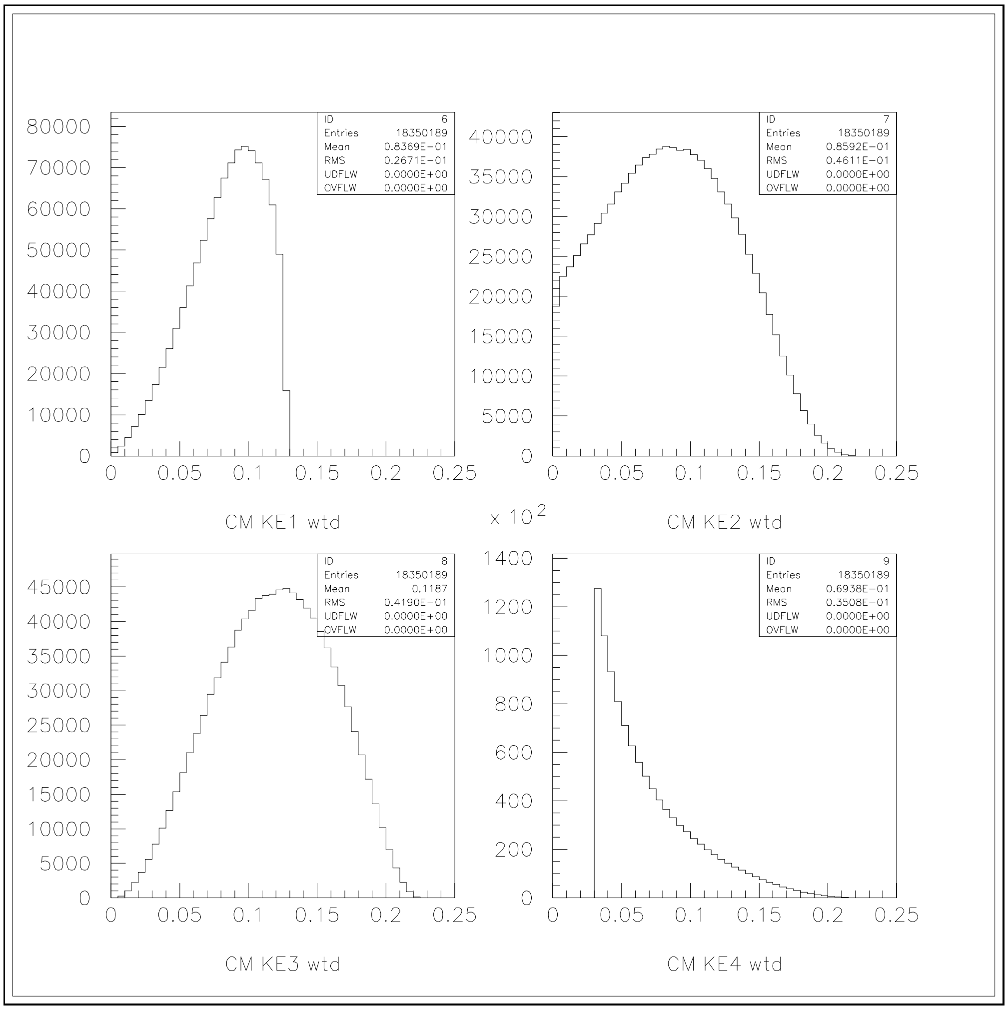


FIG. 2. Specification of decay particles CM KE.

After acceptance the particles are Lorentz transformed to the LAB and the scatter plots of the LAB $\cos\theta$ versus KE for each particle are shown in figure 3. Note there are now $10^6$ entries and most of the time $\cos\theta \approx 1$ due to $P_K$. Vetoing up stream is far less important than down stream.

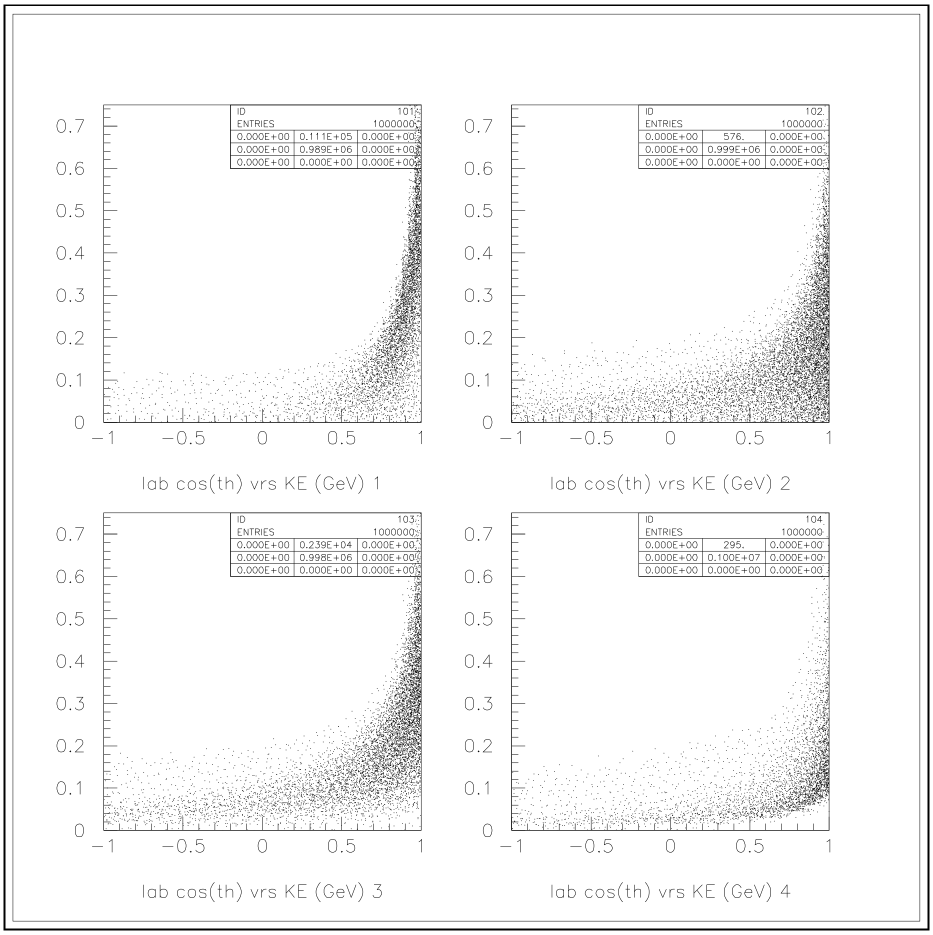


FIG. 3. Specification of decay particles LAB $\cos\theta$ and KE.

GEANT now tracks each particle through the apparatus. The default energy loss, multiple scattering, decay, and electro-magnetic packages were used while the GCALOR package was used for hadronic interactions. In figures 4-6 the energy deposited in the scintillators inside the vacuum due to either $\pi$, $e$, $\gamma$ or their decay or interaction products is shown. In figure 7 the energy deposited from any source is shown. The down stream hemisphere scintillators are the busiest as expected from the above discussion. For the $\pi$ and $e$ counters 1,2 have very similar distributions as do 3,4 and 5,6. This indicates coincidences between overlapping counters for charged particles is likely. The $\gamma$s very rarely leave energy in these scintillators. In histograms (13, 14, 23, 24, 33, 34, 43, 44) there is no suppression of channel 1 (0-0.1 MeV - misses), while in the others this channel is suppressed for clarity. The fraction of misses for each histogram is:

| | | | | | | | |
|---|---|---|---|---|---|---|---|
| 11 | 0.842 | 21 | 0.793 | 31 | 0.999 | 41 | 0.675 |
| 12 | 0.841 | 22 | 0.792 | 32 | 0.999 | 42 | 0.674 |
| 13 | 0.327 | 23 | 0.419 | 33 | 0.998 | 43 | 0.150 |
| 14 | 0.327 | 24 | 0.420 | 34 | 0.999 | 44 | 0.150 |
| 15 | 0.966 | 25 | 0.914 | 35 | 0.999 | 45 | 0.883 |
| 16 | 0.966 | 26 | 0.914 | 36 | 0.999 | 46 | 0.883 |

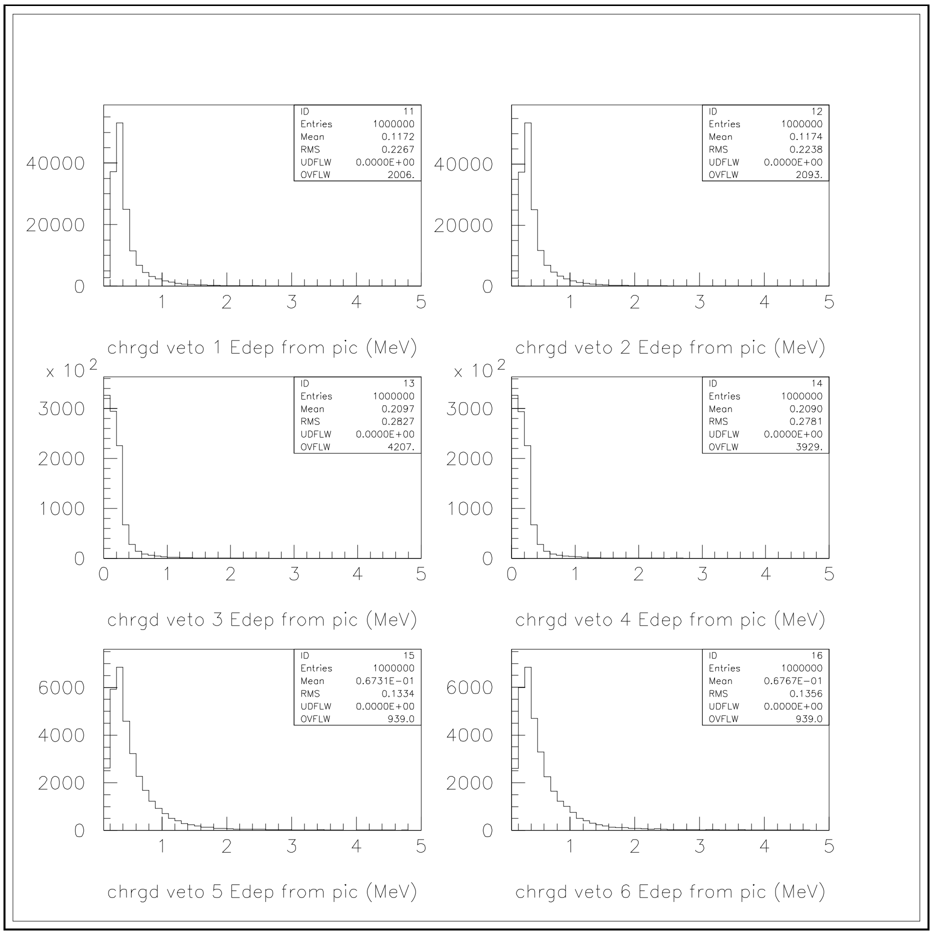


FIG. 4. Energy deposited in charged veto scintillators from $\pi^-$ and its products.

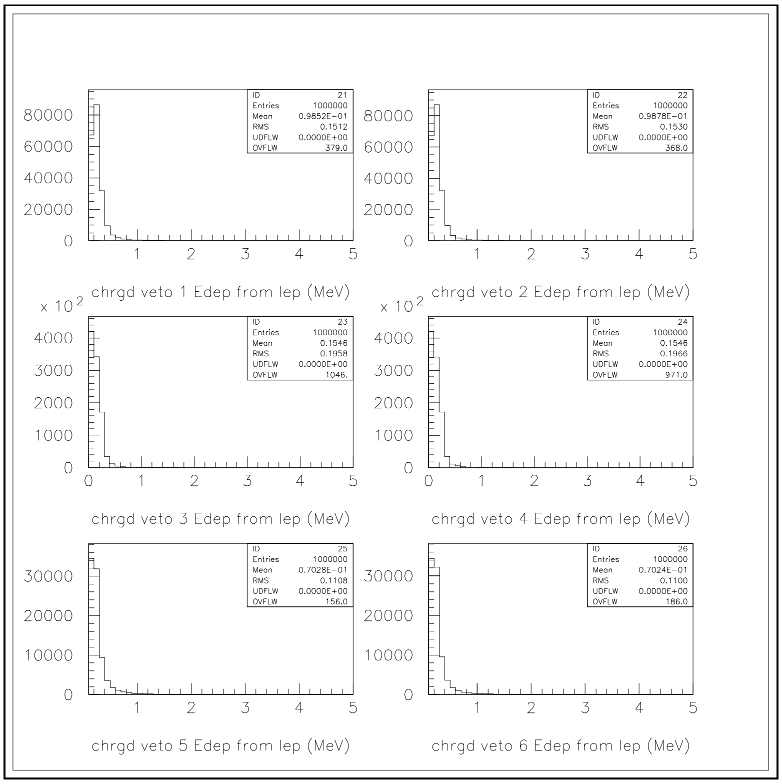


FIG. 5. Energy deposited in charged veto scintillators from $e^+$ and its products.

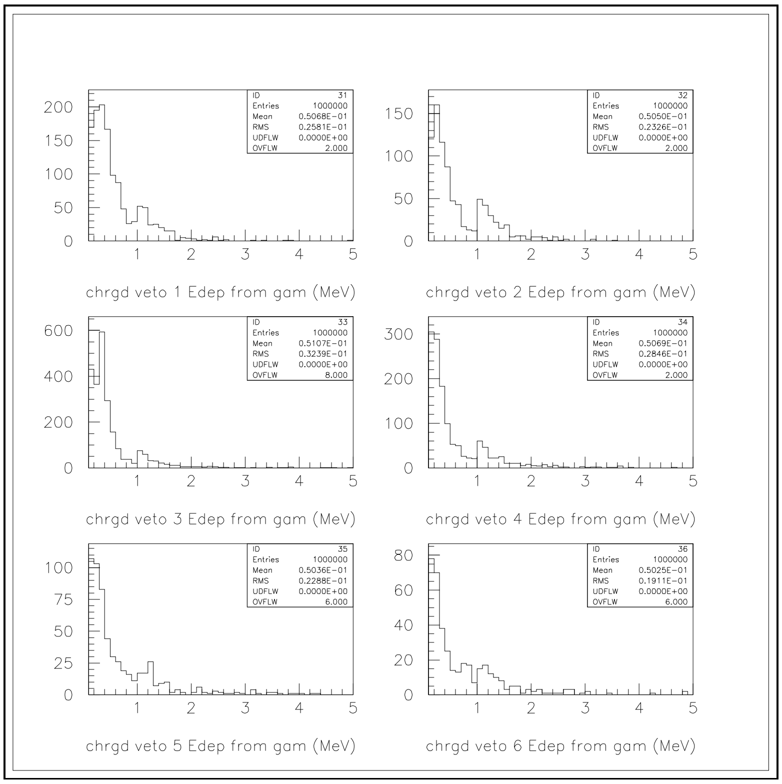


FIG. 6. Energy deposited in charged veto scintillators from $\gamma$ and its products.

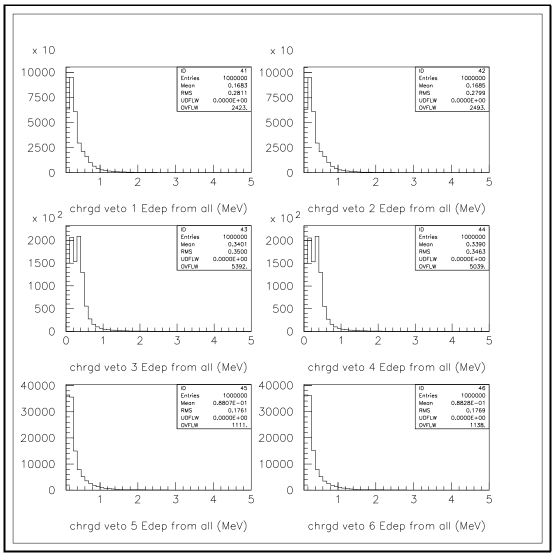


FIG. 7. Energy deposited in charged veto scintillators from all products.

In figure 8 all the spectra of figure 7 have been combined. About 5.5% of the time there is nothing in any charged veto counter nor coincidences between overlapping counters. This gives an idea of the rate at which these vetos fire from all $K_L$ decays. Most of the major decay modes also have two charged particles in the final state. For example, $BR(K_L \to \pi^{\pm}e^{\mp}\nu)/BR(K_L \to \pi^{\pm}e^{\mp}\nu\gamma) \approx 100$. So the rate in the in-vacuum vetos, assuming $10^7$ decays/s will be very high, of order, $R \approx 10^7 \times 500 \times BR(K_L \to \pi^{\pm}e^{\mp}\nu\gamma)(1. - 0.055) \approx 1.7 \times 10^7$. Segmentation is required.

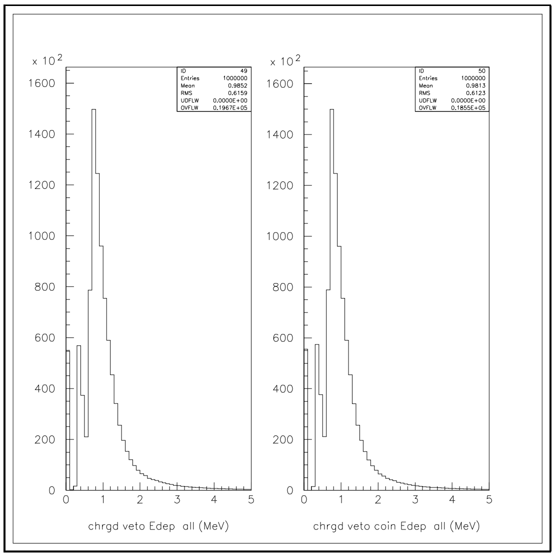


FIG. 8. Energy deposited in all charged veto scintillators from all products.

The other vetos of the detector are now examined. Figure 9 shows the energy deposited in any of the surrounding vetos outside the vacuum tank. The top histograms from left to right show the energy (0-5 MeV) deposited from the $\pi$ and its products, the $e$ and its products, the $\gamma$ and its products, and the total from all products. The bottom histograms are the same as the top except that the scale is now 0-0.25 GeV. If necessary for clarity the first channel is suppressed. The fraction of zeros in each histogram is:

51 0.691 52 0.604 53 0.593 54 0.299

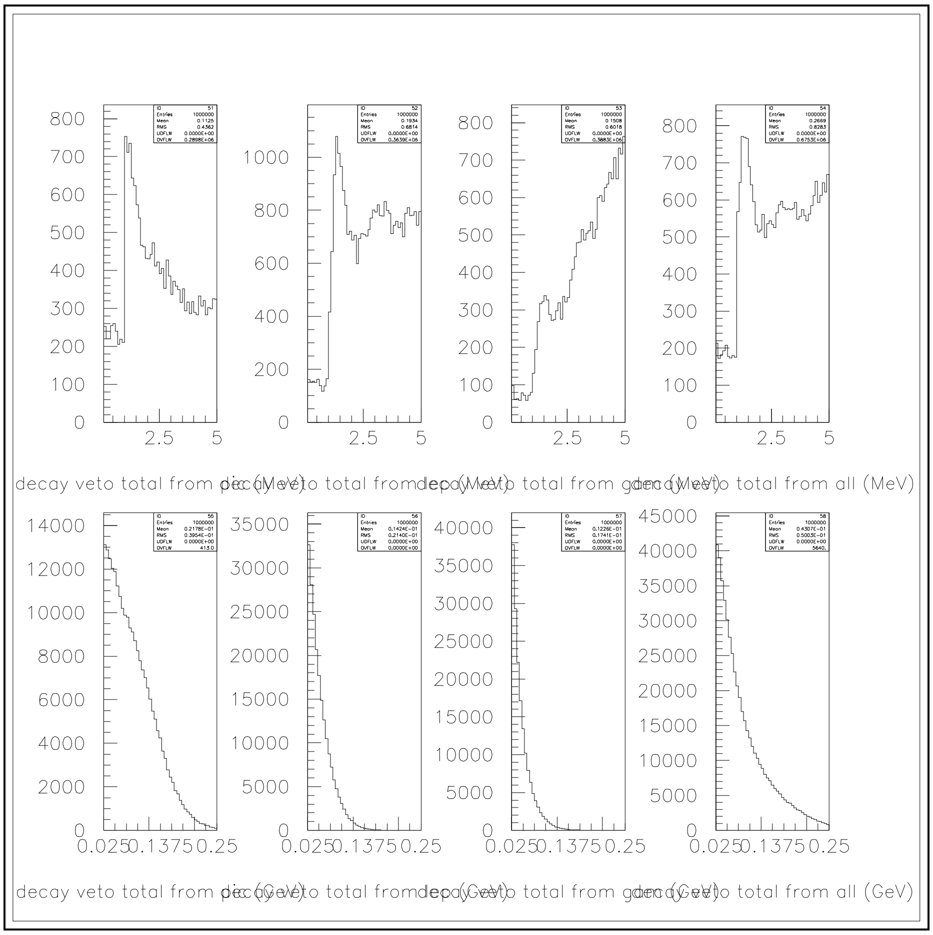


FIG. 9. Energy deposited in any veto outside of the vacuum.

In the endcap region where the preradiator and calorimeter are located no specific GEANT volumes were created . However, if particles entered this region from the beam pipe, that is through the downstream hole, then the incident KE was recorded. The assumption is that there will be scintillators or crystals lining the hole and these together with the preradiator and calorimeter will detect most of the energy. In addition if a charged particle enters the preradiator through its upstream face the incident KE was included in this veto. This is because the preradiator would have as a first counter a charged particle detector. The following figure shows the incident KE (GeV) for the $\pi$, $e$, $\gamma$, and all products. The fraction of zeros in each histogram is:

61 0.254 62 0.406 63 0.865 64 0.088

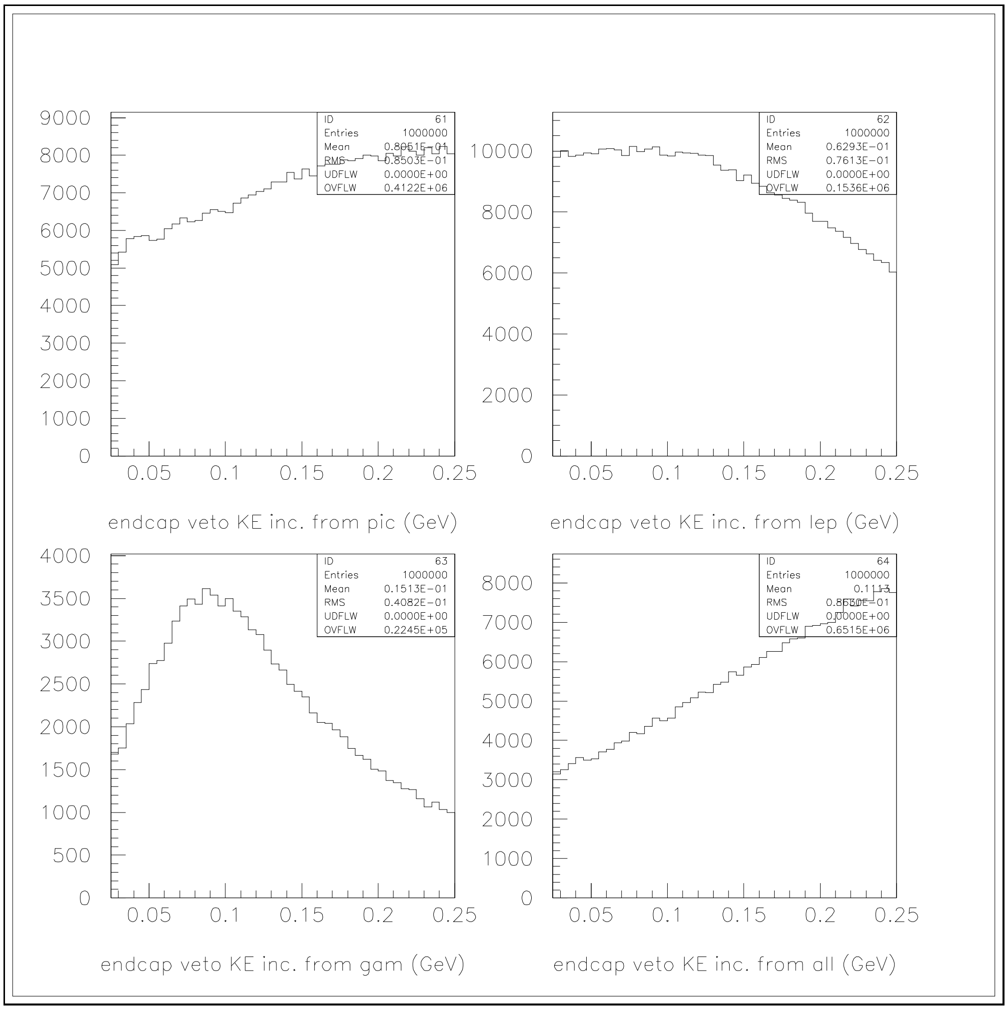


FIG. 10. Energy deposited or KE into endcap region (see text).

I then added the following additional downstream veto. If a charged particle ($\gamma$) exits the downstream end of the beam pipe with KE > 5(25) MeV, it is vetoed with 90% efficiency. This efficiency was assumed because as noted in figure 3 there are many low energy charged particles going forward. The downstream bending magnet may just turn these around rather than steer them into a veto. I keep track of whether any such particle was there in case of a good event (see below). The histograms and the zeros in each histogram after addition of this veto are:

61 0.228 62 0.370 63 0.840 64 0.066

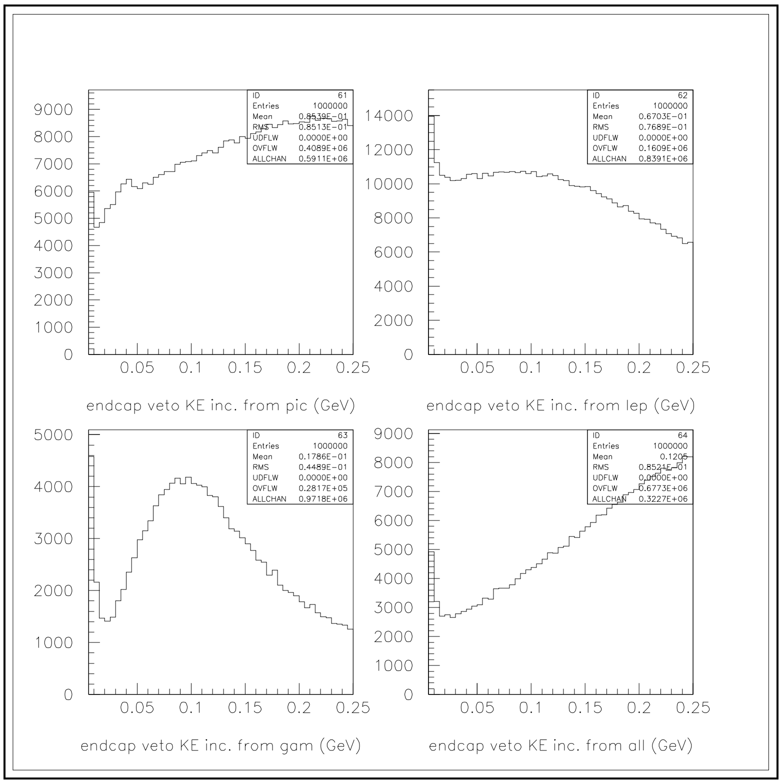


FIG. 11. Energy deposited or KE into endcap region (see text).

The following two histograms show the summed energy spectrum for all vetos between 0-5 MeV and 0.25 GeV. The misses are the number in the first channel of histogram 71; that fraction is $0.649\times10^{-3}$. After the addition of the last downstream veto the corresponding histograms shown in figure 13 were obtained. From the misses, the probability that the event is not vetoed is found to be $0.45\times10^{-4}$.

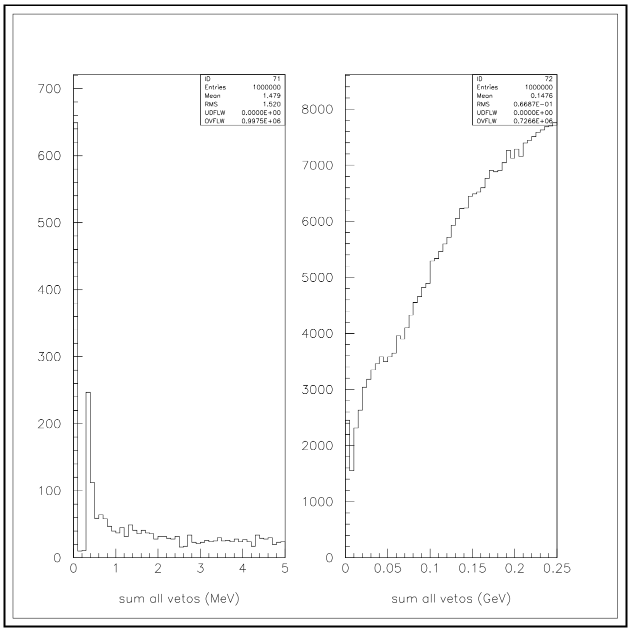


FIG. 12. Energy deposited all vetos or KE into endcap (see text).

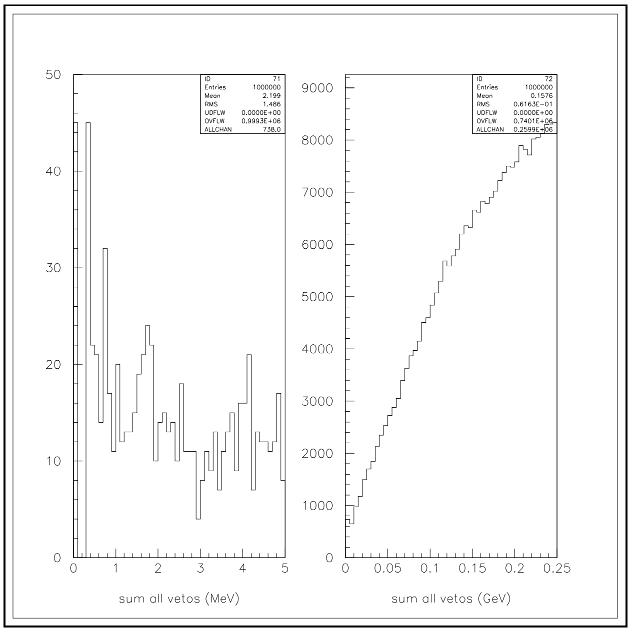


FIG. 13. As previous figure, but last downstream veto included.

Whether or not there has been any vetoing I keep track of events where exactly two $\gamma$s enter the preradiator through the upstream face. This of course excludes the probability that more than two $\gamma$s entered, but one $\gamma$ is hiding in the shower of another. The $\pi^0$ mass is subtracted from the calculated invariant mass of the $\gamma$s. Also calculated is the intersection of the $\gamma$s, the $\pi^0$ decay point. Perfect resolution was assumed. These distributions are shown in figure 14. Note that the fraction of such events is 10.7%.

The reader should note the small peak at zero missing mass (top row expanded scales). This indicates that the $\pi^- p \rightarrow \pi^0 n$ reaction is more important than $e^+$ annihilation before vetoing. About 7% of the $\pi^0$ are made in the in-vacuum veto scintillators compared to the walls of the vacuum tank. Most would not pass the "$\pi^0$" y creation point cut (see below). Also if the veto cuts were applied first (see below) the small peak disappears and any $\pi^0$ contribution is hidden in the tail of the annihilation contribution.

Cuts are now applied in two different ways. In the first way these events are subjected to the following "$\pi^0$" cuts: $|m_{12} - m_{\pi^0}| \leq 20$ MeV, $|\pi^0(x, y, z)| \leq (100, 7, 200)$ cm. After these cuts the distributions are as in figure 15. The fraction passing these cuts, $694/10^6 = 0.7\times10^{-3}$, is not so small.

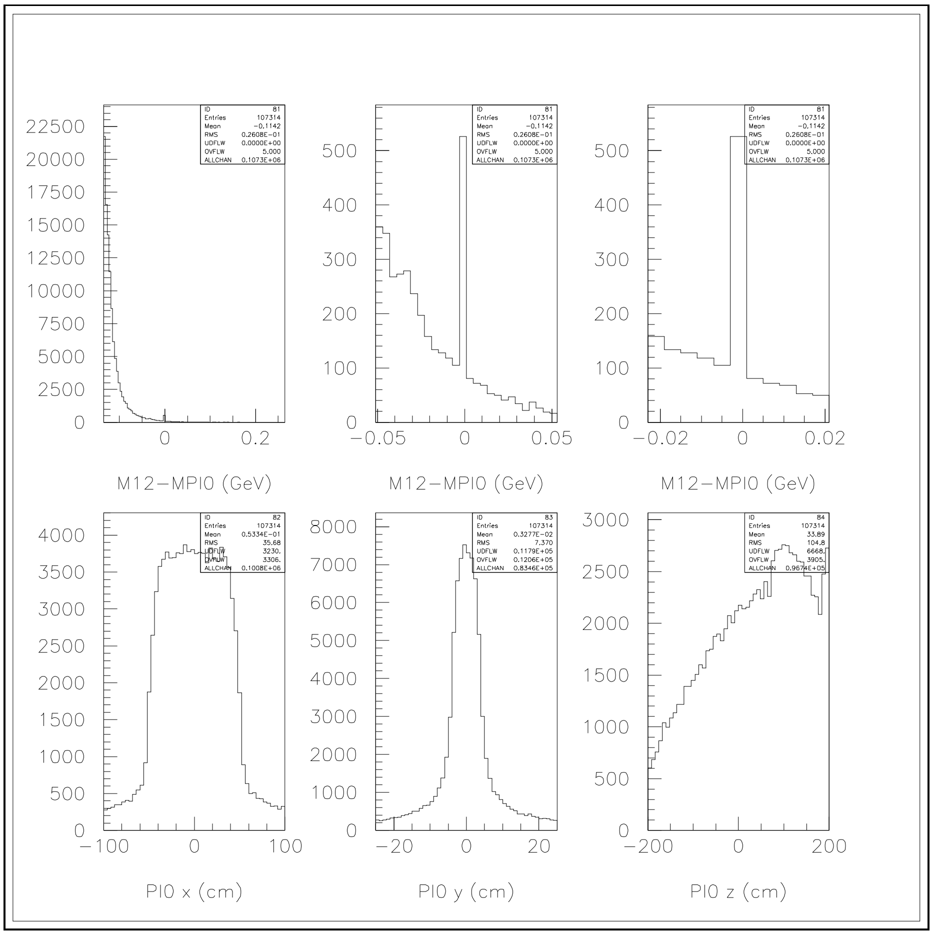


FIG. 14. $\pi^0$ variables from 2 $\gamma$ events irrespective of veto.

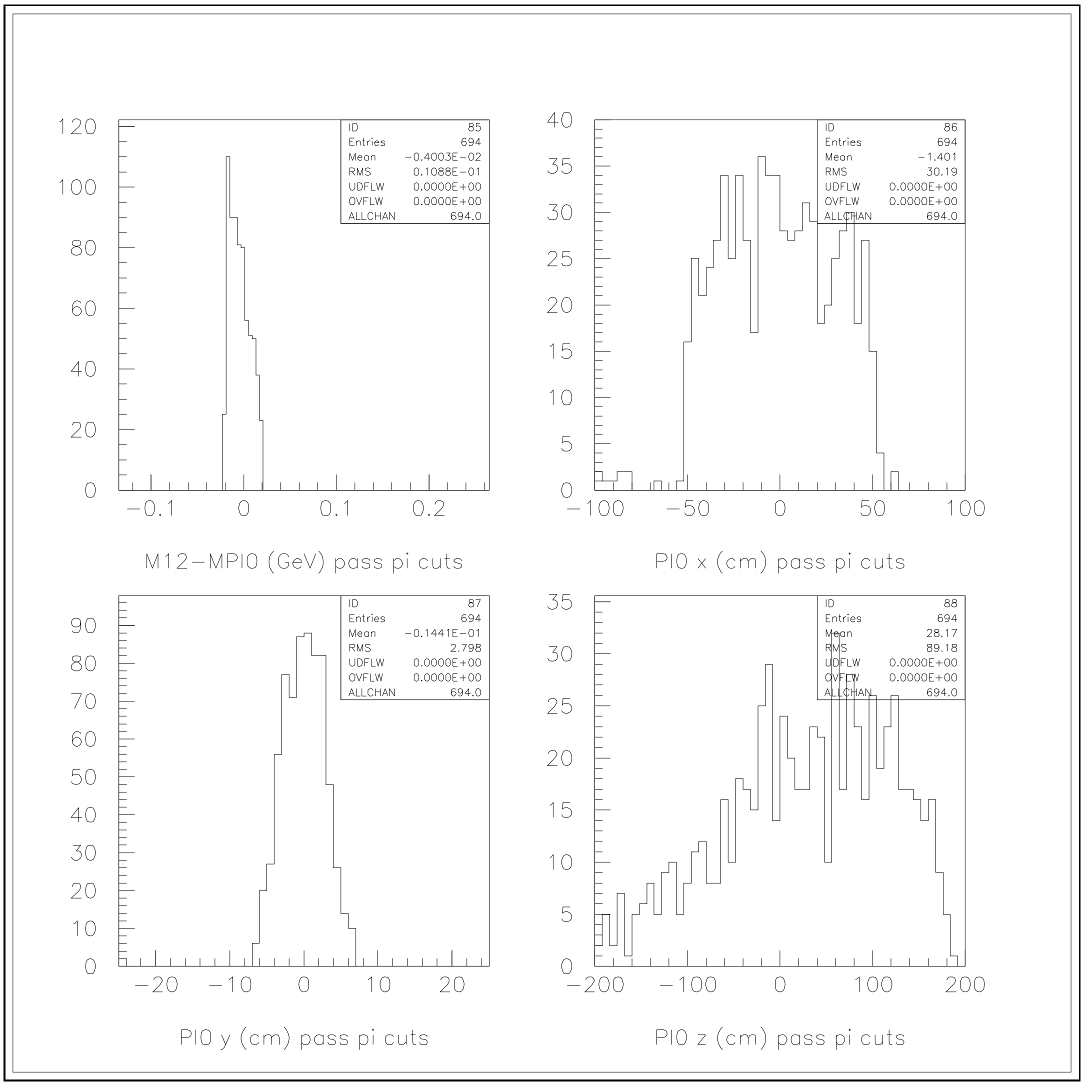


FIG. 15. $\pi^0$ variables from 2 $\gamma$ events irrespective of veto, but after $\pi^0$ cuts.

Next the event is cut if the following is true: vetos outside the vacuum have deposited energy $>$ 5 MeV or KE of charged particles entering preradiator or calorimeter $>$ 5 MeV or KE of gammas entering preradiator or calorimeter through the hole $>$ 25 MeV or KE of charged particles ($\gamma$s) exiting the downstream end of the beam pipe $>$ 5(25) MeV and it is detected with 90% efficiency or detected energy in the vacuum vetos is $>$ (0.1, 0.2, 0.3, 0.4, or 0.5) MeV. There were no events left after this cut.

In the second path the events were first subjected to veto energy cuts. For vetos inside the vacuum, the number of remaining events for a given threshold in MeV are as follows:

0.1 1 0.2 1 0.3 1 0.4 12 0.5 14

The resulting distribution for $|m_{12} - m_{\pi^0}|$ for the 0.5 MeV threshold case is shown below. These events are then subjected to the "$\pi^0$" cuts. None of the 14 events pass.

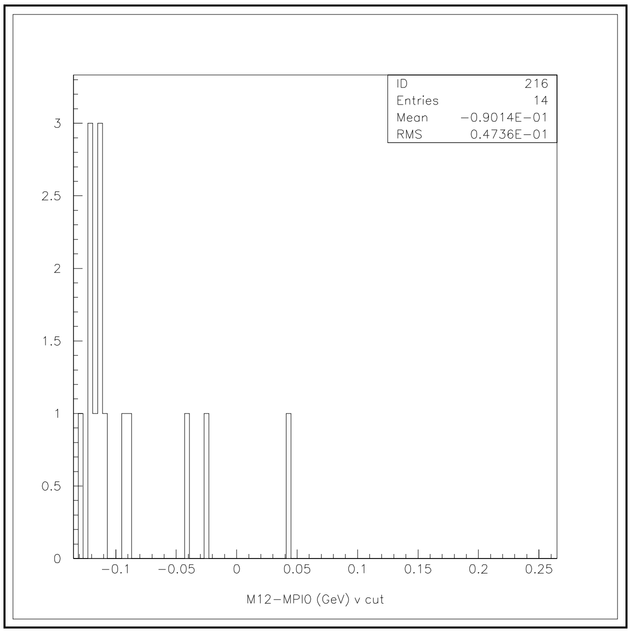


FIG. 16. Invariant $2\gamma$ mass after veto cut - threshold = 0.5 MeV.

Shown below is a scatterplot of the 14 events for $E_{\gamma 1}$ versus $E_{\gamma 2}$. There are clearly cases with two energetic gammas that can mimic a $\pi^0$.

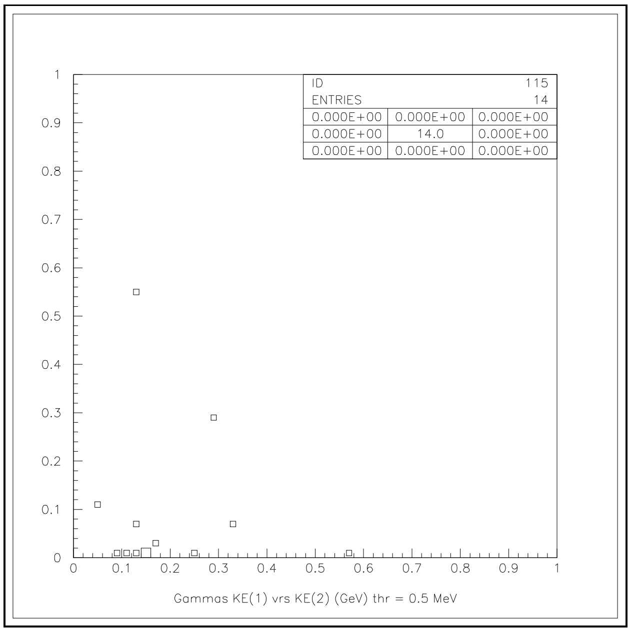


FIG. 17. $E_{\gamma 1}$ versus $E_{\gamma 2}$ in GeV.

For a run with 6 M events, there were three good events for thresholds of 0.4 and 0.5 MeV. None of these could have been vetoed by particles passing through the downstream end of the beam pipe. Just to see what happens to the probabilities I made the downstream veto 100% efficient if the charged particle ($\gamma$) KE > 25 (75) MeV. The probabilities were unchanged within the statistical error.

However, the BR of the decay considered is about $3.6\times10^{-3}$. Using $10^6$ events, at first sight, only tells us that this background is less than about 100-300 times the golden decay signal. However, from the probabilities that $2\gamma$ pass the "$\pi^0$" cuts $= 0.7\times10^{-3}$ and that the event is not vetoed $= 0.45\times10^{-4}$, the following ratio is obtained,

$$\begin{aligned}\frac{N_{BG}}{N_S} &= \frac{BR_{BG}}{BR_S}\frac{(0.45)(0.7)\times10^{-7}}{ACC_S} \\ &= \frac{3.6\times10^{-3}}{1\times10^{-11}}\frac{0.315\times10^{-7}}{ACC_S} \\ &= 11/ACC_S.\end{aligned}$$

One can conclude that this veto will **not** work.

This run took almost six hours on a 500M unix Alpha. The time can be cut by about a factor of three via stopping an event as soon as an outside of vacuum veto requirement is satisfied. The latter reduces the time to follow showers in the outside vetos. However, it would still be prohibitive to examine $10^9$ events and directly confirm my conclusion. Hopefully the probabilities herein obtained will be helpful to others running "toy" simulations. They may sustain or disprove certain assumptions. Also GCALOR doesn't include photon-nucleus reactions that may reduce the chance of a low energy photon firing a veto.

As a last exercise I wanted to see how such an in-beam veto responded to the neutron halo. Neutrons were chosen traveling parallel to the beam axis in the halo region as shown in the following figure. The region shown doesn't include halo neutrons in the vacuum pipe as nothing happens to them. All reaction products were stopped after exiting the vacuum region. There will be some back scatter, but that effect is ignored here.

For various neutron momenta, I give the fraction of events with more than 0.1 MeV deposited in the in-vacuum vetos. The halo contains about $10^7$ n/s of rapidly declining momenta so these fractions, out of $10^4$ cases are a guide to the rate at which these vetos fire. The rates are low ($< 10^4$/s).

| $veto$ | $0.1 GeV/c$ | $0.5 GeV/c$ | $1 GeV/c$ | $3.5 GeV/c$ |
|---|---|---|---|---|
| 1 | 0.0 | 0.0059 | 0.0088 | 0.0182 |
| 2 | 0.0 | 0.0062 | 0.0090 | 0.0185 |
| 3 | 0.0001 | 0.0078 | 0.0113 | 0.0344 |
| 4 | 0.0001 | 0.0068 | 0.0106 | 0.0337 |
| 5 | 0.0004 | 0.0145 | 0.0230 | 0.0382 |
| 6 | 0.0003 | 0.0151 | 0.0225 | 0.0383 |

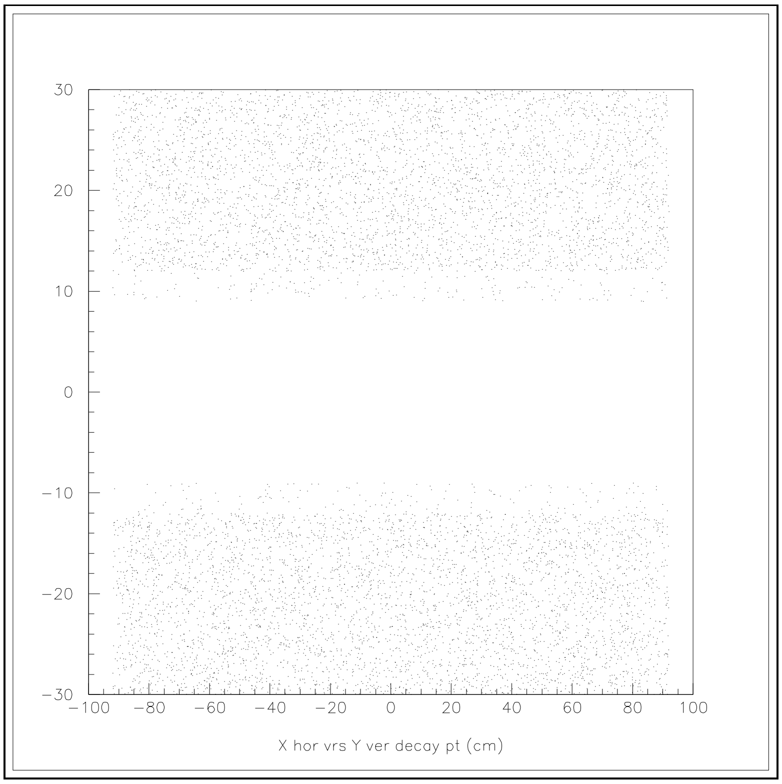


FIG. 18. Halo neutrons x vrs y.

It will require only a small geometry modification to see what some other veto setup can do. If some one has a scheme they would like tried out, please email me.